JOURNAL OF GEOPHYSICAL RESEARCH, VOL. 92 NO. A8, PAGES 8545-8557, AUGUST 1 1987

CHARACTERISTICS OF THE MARSLIKE LIMIT OF THE VENUS-SOLAR WIND INTERACTION

J. G. Luhmann,[1] C. T. Russell,[1] F. L. Scarf,[2]
L. H. Brace,[3] and W. C. Knudsen[4]

Abstract. Many authors have already noted that Mars' interaction with the solar wind may be like Venus', e.g., that of a supermagnetosonic plasma flowing past an effectively unmagnetized body having an ionosphere. However, at Mars, the incident solar wind dynamic pressure usually exceeds the peak ionospheric plasma pressure, while at Venus this condition prevails only when the incident dynamic pressure is extraordinarily high. With the aim of predicting what might be expected at Mars, this study examines the subset of Pioneer Venus Orbiter observations obtained during intervals of extremely high solar wind dynamic pressure. The characteristic features of this limit of the Venus-solar wind interaction include a bow shock position that is not notably different from the norm, altitude profiles of the dayside upper ionosphere density without a sharp increase in gradient at the ionopause, and dayside electron temperatures that rapidly increase with altitude to consistently exceed the temperatures above 200 km which are present for lower solar wind pressures. Depleted nightside ionosphere densities, and a large-scale horizontal magnetic field in both the dayside and nightside ionospheres, are among the previously identified responses to high dynamic pressure. Here, emphasis is placed on the dayside ionosphere because some data are available for the dayside Martian ionosphere from the Viking mission. The density and ion temperature trends are found to be similar to those seen in the Viking data. Overall, the Venus observations at high dynamic pressure provide a framework for reassessing the available Mars observations. In particular, this study shows that the observed absence of a distinct ionopause "cutoff" in the dayside plasma density gradient cannot be construed as evidence for an intrinsic magnetic field which stops the solar wind at higher altitudes. Similarly, the rules of thumb that the electron temperature is given by twice the ion temperature and that the ionospheric magnetic field pressure can only double the total ionospheric pressure, which have been applied to assess Mars' ability to standoff the solar wind, are not justified. Observations at Venus thus illustrate the expected modification of the common pressure balance picture of the solar wind interaction at an unmagnetized planet with a weak ionosphere. The available Mars observations appear to be consistent with this modified picture.

[1]Institute of Geophysics and Planetary Physics, University of California, Los Angeles.
[2]TRW Space and Technology Group, Redondo Beach, California.
[3]NASA Goddard Space Flight Center, Greenbelt, Maryland.
[4]Knudsen Geophysical Research, Monte Sereno, California.

Paper number 7A8965.
0148-0227/87/007A-8965$05.00

Introduction

Ironically, less is known about the intrinsic magnetic field of our near neighbor Mars than is known about the fields of the distant giant planets. The only relevant measurements that are currently available consist of ionospheric data obtained by spacecraft en route to deliver landers, and of higher-altitude data from orbiters with limited lifetimes which never encountered the ionosphere. While these observations are enough to rule out a magnetic field of the strength producing the known planetary magnetospheres, there remains a continuing controversy over whether the planetary magnetic field is sufficient to affect the solar wind interaction with Mars. Whereas the prospect of resolving this question by in situ measurements in the near future is uncertain, our ability to assess the situation is greatly improved by the availability of the extensive data obtained at Venus. These data allow one to examine in detail the plasma and field in the vicinity of an obstacle consisting of a planet with a substantial atmosphere but negligible intrinsic field. However, comparisons of the characteristics of the Venus data with the limited observations from the Mars and Viking spacecraft encounters have led to arguments both for [cf. Dolginov, 1978; Slavin and Holzer, 1982] and against [cf. Russell et al., 1984] a planetary field of any consequence.

Several of the analyses concerned with Mars' intrinsic magnetic field have concentrated on the interplanetary features of the solar wind interaction. At the outer boundary of the interaction region, the bow shock positions observed by the MARS and Mariner spacecraft provide a measure of the obstacle size. Taking advantage of the gasdynamic models of Spreiter and Stahara [1980], Slavin and Holzer [1983] used the relationship between the shock and obstacle shapes to deduce the location of the surface that deflects the solar wind plasma. By applying the knowledge that at Venus, the solar wind appears to be diverted around a boundary where the incident solar wind dynamic pressure is balanced by the equivalent ionospheric thermal pressure [cf. Brace et al., 1983; Phillips et al., 1984], these authors concluded that the required Mars obstacle is larger (by several hundred kilometers at the nose) than the pressure balance surface inferred from the ionospheric observations. Their interpretation was that an intrinsic magnetic field stands off the solar wind at Mars. However, it is also known from the Venus observations that the bow shock can be anomalously distant due to mass loading of the solar wind plasma [Slavin et al., 1980; Mihalov et al., 1982; Alexander et al., 1986]. Mass loading occurs because planetary ions are produced from the neutral exosphere that extends into the magnetosheath. This consideration seri-

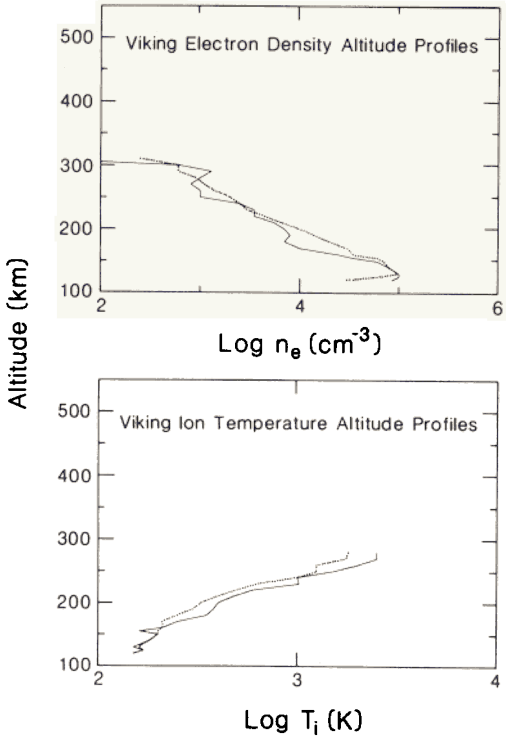

Fig. 1. Altitude profiles of (top) electron density and (bottom) ion temperature measured along the Viking spacecraft trajectory by Hanson et al. [1977]. The solid lines show the Viking 1 data; the dotted lines show the Viking 2 data.

ously undermines the traditional method of obstacle determination by gasdynamic modeling [cf. Belotserkovskii et al., 1987].

In another study utilizing the gasdynamic model, Russell et al. [1984] demonstrated that the Soviet MARS spacecraft magnetic data were consistent with a draped magnetosheath field interpretation with no planetary field. In their study, the obstacle size was inferred to be of the same order as Slavin and Holzer's [1982] estimate. Their deduction of the obstacle, of course, similarly suffered from its neglect of mass loading effects on the magnetosheath flow.

MARS spacecraft magnetic field observations of the Mars magnetotail provided an independent test of intrinsic field strength [Dolginov, 1977]. However, the limited amount of data obtained in the wake, and their complexity, leave room for uncertainty regarding an interplanetary (Venus-like) or intrinsic origin of the structure [cf. Vaisberg and Smirnov, 1986].

Other arguments concerning the nature of the Mars-solar wind interaction and the role of an intrinsic field have focused on Mars' ionospheric properties, but the ionospheric measurements from the two Viking spacecraft have likewise been a source of ambiguity. Hanson et al. [1977] obtained the two altitude profiles (along the spacecraft orbit) of electron density and ion temperature in the dayside ionosphere shown in Figure 1. One of the electron density profiles appeared to include a reduction in scale height near ~300 km altitude, reminiscent of a Venuslike ionopause, but the other did not. Both ion temperature profiles exhibited increases with altitude that could not be explained by solar heating alone. These profiles could be modeled only by including the combination of a topside heat source and a nearly horizontal magnetic field similar to that occasionally observed in the Venus ionosphere [Chen et al., 1978; Johnson, 1978; Rohrbaugh et al., 1979]. Although the electron temperature was not measured, one of the key results of these observations was that for "reasonable" estimates of the electron temperature (about twice the ion temperature), the maximum ionospheric plasma pressure is less than the typical dynamic pressure of the incident solar wind ($\sim 1 \times 10^{-8}$ dyn cm^{-2}) by a factor of at least 2 [cf. Slavin and Holzer, 1982]. In contrast, Venus' ionosphere pressure usually exceeds that of the incident solar wind.

In view of the difference between the strengths of the ionospheres of Mars and Venus, it is most appropriate to compare the Mars results with the specific subset of the Venus observations for which the solar wind dynamic pressure exceeds the Venus ionospheric pressure rather than with a typical data set. The purpose of this report is to focus on the special behavior of Venus' solar wind interaction in this "overpressure" situation, with the intent of characterizing the closest possible empirical model for Mars.

Typical Venus-Solar Wind Interaction

For perspective, it is useful to briefly review what is known about the normal and high dynamic pressure interactions at Venus. The Venus-solar wind interaction under typical conditions has been described by many authors (see, for example, several chapters in Venus, edited by Hunten et al. [1983]). In this scenario, nearly dissipationless currents flowing in a thin layer of the collisionless upper ionosphere in the vicinity of the pressure balance surface produce magnetic fields that deflect the solar wind plasma flow, and with it, the interplanetary magnetic field. The analogy of a superconducting sphere in the flowing plasma is often invoked to describe this condition which prevails most of the time at Venus [cf. Johnson and Hanson, 1979].

Some of the observed departures from this superconducting sphere analogy can be attributed to mass loading of the magnetosheath by planetary ions. The effects of this process are evident in both the bow shock position (which is more distant than expected for an obstacle the size of the pressure balance surface, as mentioned earlier), and in the existence of an induced magnetotail with lobe polarities determined by the draped interplanetary field orientation [cf. Saunders and Russell, 1986]. The ionosphere below the shielding current layer also exhibits behavior unlike that of the perfectly isolated interior of a superconductor. Small-scale magnetic structures called "flux ropes" [cf. Elphic and Russell, 1983], which appear within the ionosphere down to at least the Pioneer Venus Orbiter periapsis altitude of ~150 km, provided one indication of imperfect shielding.

With regard to the ionospheric plasma itself, Cravens et al. [1980] used Pioneer Venus observations of the ion densities to demonstrate that the observed ion and electron temperatures were not consistent with a model that assumed heating of an isolated atmosphere by solar EUV alone.

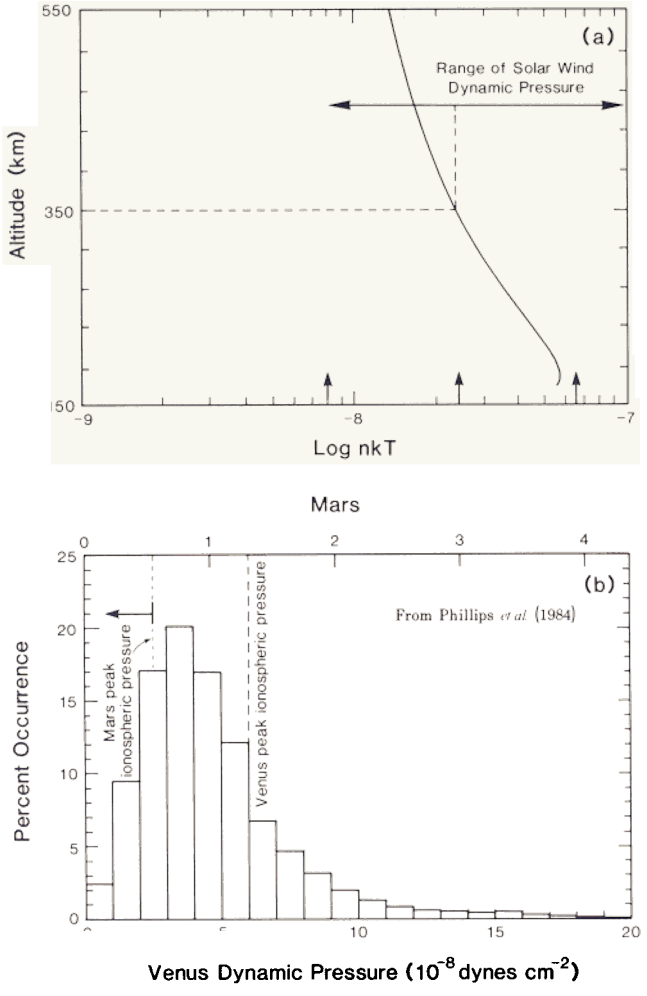

Fig. 2. (a) Altitude profile of thermal pressure (nkT) in the Venus subsolar ionosphere according to the Pioneer Venus Orbiter observations of Miller et al. [1984]. The range of the incident solar wind dynamic pressure is indicated at the top. The dashed line illustrates how the ionopause altitude can be inferred from the incident dynamic pressure under normal conditions. Three arrows on the horizontal axis are explained later in the text. (b) Statistics of solar wind dynamic pressure during 1980 at Venus as measured by the Pioneer Venus plasma analyzer [from Phillips et al., 1984].

These authors found that both small, irregular ionospheric magnetic fields and a heat source at the upper boundary of their model were required to bring the average observations into closer agreement with theory. Thus even for typical solar wind conditions, the Venus interaction is not without complications introduced by the interplanetary plasmas and fields. Nevertheless, other considerations come into this picture when the ionospheric pressure is insufficient to stand off the solar wind dynamic pressure at altitudes where collisions can be neglected.

Between the state described above and the Marslike overpressure state, there is a state with high (but not excessive) dynamic pressure where effective shielding currents still flow but are no longer confined to the collisionless regions of the ionosphere. This state has received considerable attention [cf. Luhmann et al., 1984; Cravens et al., 1984; Phillips et al., 1984] because it is relatively simple to understand in terms of a picture where the combination of ionospheric convection and diffusion redistribute the overlying magnetosheath magnetic flux.

The state of magnetization of the subsolar ionosphere has been found to be sensitive to two things: the boundary condition on the field at the top of the ionosphere (including field magnitude and boundary altitude) and the vertical velocity [cf. Luhmann et al., 1984; Cravens et al., 1984; Phillips et al., 1984]. The magnetic field diffuses across the ionopause from the magnetosheath and once in the ionosphere is convected downward by the ionospheric plasma that is formed at high altitudes but recombines at low altitudes. Variations in the height of the ionopause affect both the rate of diffusion and downward convection, so that the largest ionospheric fields are associated with the lowest ionopauses. Phillips et al. [1984] have used the vertical ionospheric velocity described by Cravens et al. [1984] to model the variation of the ionospheric field with altitude. The fixed velocity profile, together with the upper boundary altitude and field magnitude, usually reproduces the observed ionospheric field. However, in this intermediate limit, where this diffusion/convection model is valid, the ionosphere is only slightly affected by the presence of the magnetic field. As Cravens et al. [1984] and Shinagawa et al. [1987] have shown, as the ionospheric magnetic field grows, it must ultimately influence the vertical drift velocity.

Previously Identified Attributes of the Venus High Dynamic Pressure Interaction

The plasma pressure in the subsolar ionosphere of Venus has an altitude profile that was determined by Miller et al. [1984] from retarding potential analyzer measurements on the Pioneer Venus Orbiter. In Figure 2a, the range of the subsolar ionospheric plasma pressure, as it might appear along the spacecraft trajectory, is compared with the range of incident solar wind pressures. (Here and elsewhere, the solar wind dynamic pressures are derived from measurements by the Ames plasma analyzer on the Pioneer Venus Orbiter, courtesy of J. D. Mihalov and A. Barnes.) For comparison, Figure 2b from Phillips et al. [1984] is reproduced to emphasize that the average dynamic pressure at Venus is near 3.5×10^{-8} dyn cm^{-2}, but enhancements of up to an order of magnitude greater occasionally occur. Consequently, the solar wind stagnation pressure ($\sim$0.84 times the actual pressure) exceeds the nominal Venus ionosphere peak pressure ($\sim 5.7 \times 10^{-8}$ dyn cm^{-2}) $\sim$15% of the time, during which the Venus solar wind interaction becomes more like that of Mars. For comparison, the upper scale in Figure 2b indicates how the dynamic pressure is reduced by its radial expansion from Venus to Mars. A dotted line shows the peak Martian subsolar ionospheric pressure inferred by Slavin and Holzer [1982] from the Viking data, and the assumption that the electron temperature is twice the ion temperature. In contrast to Venus, in which the solar wind pressure exceeds the peak ionosphere pressure

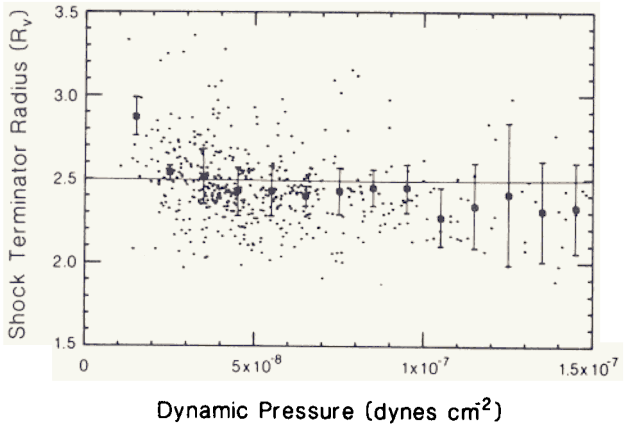

Fig. 3. Bow shock positions extrapolated to the terminator plane as a function of the prevailing solar wind dynamic pressure. The data are a combination of the set used by Tatrallyay et al. [1983] and more recent observations.

only about 15% of the time, the solar wind pressure at Mars is expected to be greater than the peak ionospheric pressure 85% or more of the time. Of course, this comparison should be qualified in that the Mars ionosphere data were obtained near solar minimum when the ionosphere was at its weakest, while the Venus observations represent solar maximum conditions.

One of the first questions that needs to be answered is whether the apparent size of the obstacle as inferred from the bow shock position is affected when the solar wind pressure exceeds the ionospheric pressure. If substantial absorption of the incident solar wind plasma occurs, one might expect the apparent obstacle to become smaller as the amount of deflected solar wind plasma in the magnetosheath diminishes, or to disappear altogether as in the lunar-solar wind interaction which produces no bow shock. However, as Figure 3 indicates, the obstacle size at Venus as reflected in the terminator distance of the bow shock is not significantly different from the norm for dynamic pressures exceeding the nominal peak ionosphere pressure [see also Tatrallyay et al., 1983]. This behavior suggests that the effective obstacle at Venus is about the size of the planet, even in the limit of solar wind overpressure. The weak correlation between shock radius and solar wind pressure seen at low pressures is probably due to the correlation of low dynamic pressures with low Mach numbers in the solar wind. Mach number does control the shock size at Venus at low Mach numbers.

Although the bow shock position at Venus is not greatly altered during the high dynamic pressure conditions, it is known that the ionopause position responds by dropping to its limiting altitude of ~220 km [Brace et al., 1983]. Figure 4 illustrates the altitude of both the pressure balance surface (between the magnetic field and plasma) and of the 100 cm^{-3} electron density level (the definition for the ionopause employed by Theis et al. [1980]) as a function of the total pressure at the pressure balance surface. The latter was shown by Phillips et al. [1984] to reflect the normal component of the incident solar wind dynamic pressure. The reason for the 220-km-altitude limit of the ionopause at high dynamic pressures has not been discussed in the literature. Related to this "minimum ionosphere" condition, one finds both a large-scale, nearly horizontal magnetic field of up to ~150 nT inside the dayside ionosphere [cf. Luhmann et al., 1980], and an apparent reduction of the high-altitude transport of dayside ionosphere plasma to the nightside [cf. Cravens et al., 1982]. The latter has been inferred from the "disappearing" nightside ionosphere phenomenon observed by the Pioneer Venus Orbiter. The nightside ionospheric density data from the Langmuir probe gave rise to this terminology because they showed density profiles that were severely depleted compared to normal profiles. An unusually strong (tens of nanoteslas) and horizontal ionospheric magnetic field is often associated with these depleted nightside ionospheres.

The behavior of the dayside ionosphere during overpressure conditions has not been specifically examined, although Elphic et al. [1984] carried out a statistical study of Pioneer Venus Langmuir probe data which indicated that the associated ionospheric magnetic fields generally had no effect on the ionospheric density and electron temperature. This negative result is partially attributable to their method of analysis, which involved less stringent selection criteria than are used here, and to the restriction of their study to altitudes below 200 km.

Observations of the Venus-Solar Wind Interaction in the Overpressure Limit

A number of authors have considered that a significant fraction of the incident solar wind

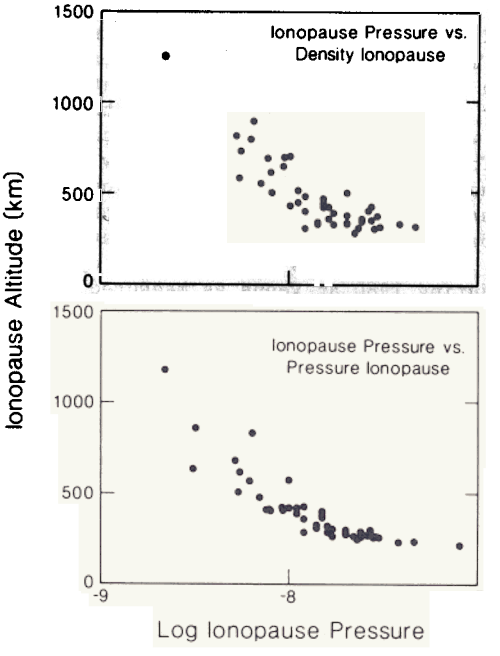

Fig. 4. Altitude of the ionopause versus the total local pressure (plasma plus magnetic field), which is approximately equal to the solar wind dynamic pressure. Both pressure balance and density ionopauses are shown [cf. Phillips et al., 1984].

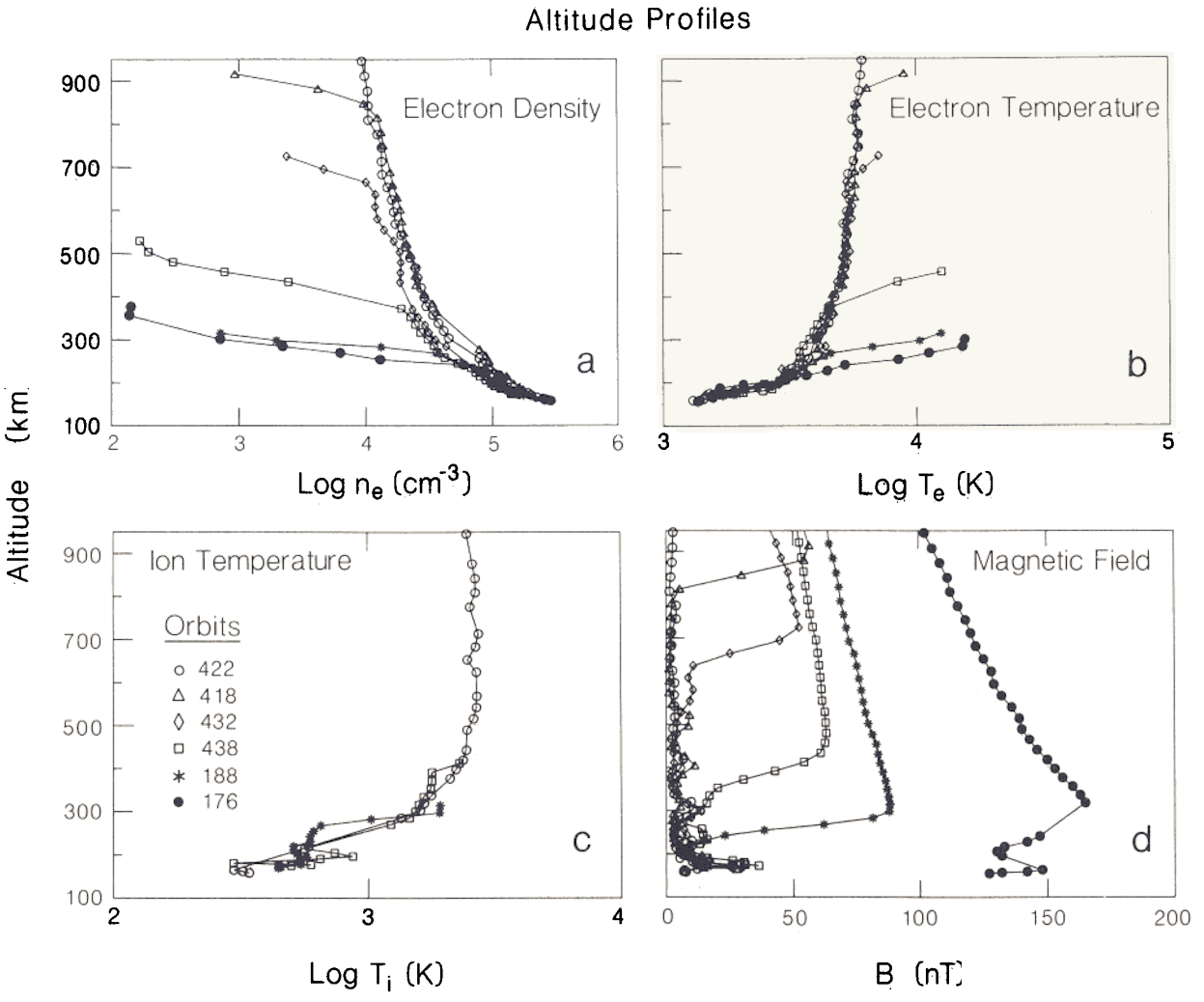

Fig. 5. Examples of altitude profiles of various quanties measured along the Pioneer Venus trajectory. These were selected from the subsolar data to illustrate the respons of the ionosphere to increasing solar wind dynamic pressures. (Similar variations with solar zenith angle also occur.) The different symbols identify the different orbits. Only the outbound leg of each orbit is shown because it is closer to a true altitude profile sample than the inbound leg. (a) Ionosphere densities measured by the Langmuir probe. (b) Electron temperatures from the Langmuir probe. (c) Ion temperatures measured by the retarding potential analyzer. (d) Magnetic field magnitude.

must be absorbed by Venus' atmosphere at times of high solar wind dynamic pressure. In particular, Gombosi et al. [1981] argued that charge exchange of solar wind protons with planetary neutrals would completely replace any solar wind protons reaching ~215 km altitude with heavy planetary ions. The absorption of the solar wind should heat the dayside atmosphere and ionosphere as the soft proton influx deposits its energy in a cascade of charge exchange collisions and ionizing Coulomb collisions. The ion temperature, in particular, should show evidence of this energy deposition. Moreover, the deflection of the solar wind plasma in the magnetosheath should lessen as the amount of solar wind plasma that must flow around the flanks of the obstacle decreases. However, we know from the aforementioned observations that, under overpressure conditions, the bow shock does not move very far from its usual position. This means that the planet must somehow compensate for the apparent weakness of its ionosphere and continue to deflect the bulk of the incident solar wind. An examination of the Pioneer Venus ionospheric data for orbits during which extraordinary solar wind conditions prevailed can show how the planet accomplishes this.

The examples of Pioneer Venus ionospheric profiles in Figure 5 were selected because they illustrate the response of the subsolar ionosphere to increasing solar wind dynamic pressure. These, and all of the ionospheric data used in the present study, come from the Langmuir probe, retarding potential analyzer, magnetometer, and plasma wave detector contributions to the Universal Access Data System (UADS) data base, which contains 12-s averages of the Pioneer Venus Orbiter data from the hour surrounding periapsis. It should be noted here that these profiles are not true altitude profiles in the sense that the spacecraft usually travels ~1000 km horizontally during the spacecraft encounter with the ionosphere. However, the similarity of the data ob-

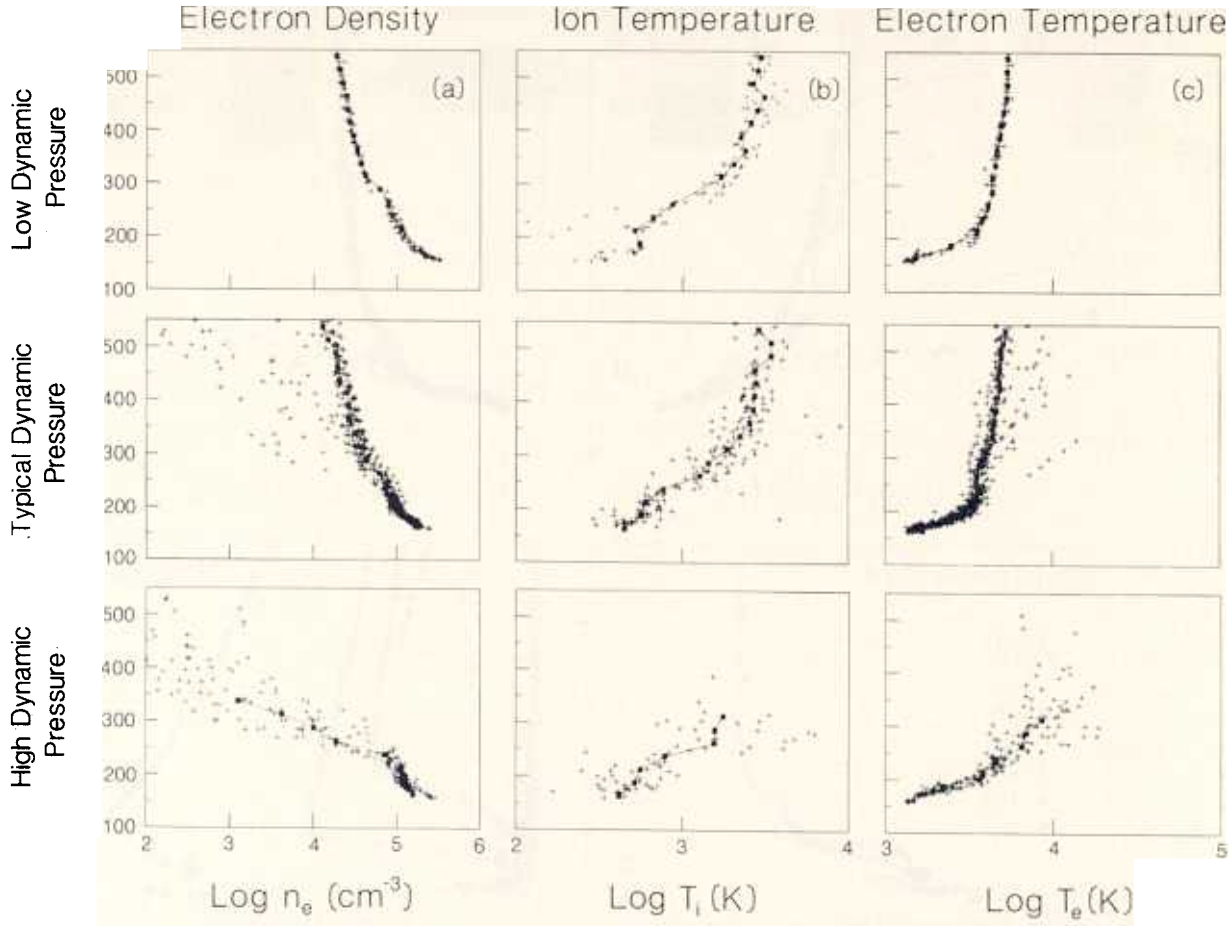

Fig. 6. UADs data for the three classes of solar wind dynamic pressure and their median altitude profiles. (The median dynamic pressures are indicated by arrows in Figure 2a). (a) Ionospheric density. (b) Ion temperature. (c) Electron temperature

tained on the inbound and outbound segments of these orbits suggests that altitude variations dominate solar zenith angle or latitudinal variations. (The two orbit segments intersect different solar zenith angle ranges.) Nevertheless, only outbound segments are used here because the outbound trajectory traverses the smaller horizontal distance.

As previously noted [cf. Brace et al., 1983], the ionospheric plasma density decreases rapidly in the subsolar region above an altitude where the thermal pressure is equal to the normal component of the incident solar wind pressure. The altitude of this sharp "ionopause," seen in the high-altitude portions of the Langmuir probe electron density profiles in Figure 5a, is very responsive to changes in solar wind pressure under normal solar wind conditions. But this behavior is no longer observed when the projected pressure balance surface is below ~220 km [Phillips et al., 1984], corresponding to dynamic pressures of 4×10^{-8} dyn cm^{-2} and above. Under such conditions the ion density consistently assumes the behavior described by the lowest and most eroded profile in Figure 5a. Simultaneous retarding potential analyzer ion temperature profiles for several of these examples, which are given in Figure 5b, exhibit no clear evidence of a systematic variation as the density profile changes. In contrast, the Langmuir probe-derived electron temperature profiles in Figure 5c indicate that localized heating occurs within the upper electron density gradient, and that this heating extends to at least ~ 200 km when the ionopause has been forced to its minimum (220 km) altitude. It should be mentioned here that these electron temperature measurements may be affected by the nonisotropic and non-Maxwellian nature of the electrons in the region of the ionopause gradient. Figure 5d, which shows the corresponding magnetic field profiles, is included to illustrate the external conditions in the magnetosheath for these examples.

To better characterize the high dynamic pressure interaction, a set of about 50 orbits with periapsis in the subsolar range (solar zenith angles $\lesssim 30°$) was selected to represent the full range of solar wind dynamic pressures. These orbits were divided into three categories representing low, typical and high dynamic pressure conditions, and their corresponding median dynamic pressures are marked by the arrows along the axis in Figure 2a. Figure 6 shows the median altitude profiles of the basic ionospheric quantities for these classes, together with the complete collection of individual data points. Figure 7 summarizes Figure 6 by superposing the median profiles. In this display, several ionospheric features of the high dynamic pressure interaction stand out. As noted before, the electron density profiles (Figure 7a) reach a limiting shape. In these pro-

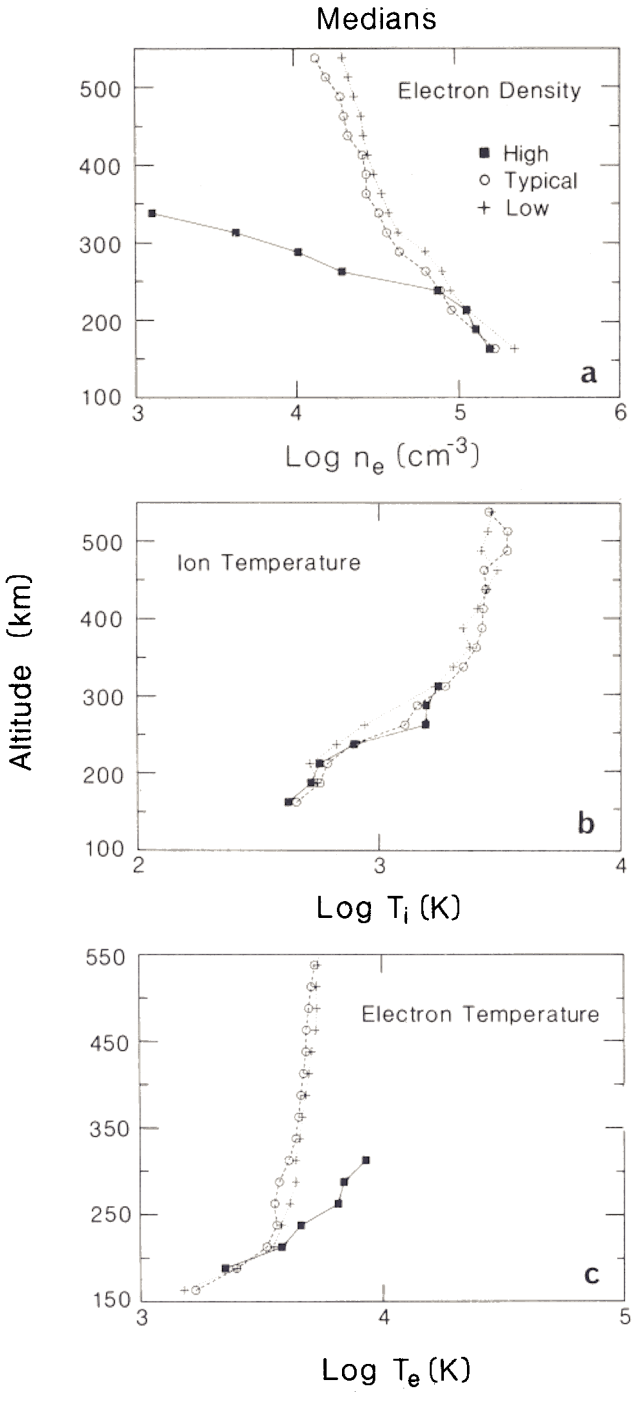

Fig. 7. Comparisons of the medians from Figure 6. (a) Ionospheric density. (b) Ion temperature. (c) Electron temperature.

files, there is no sudden steepening of the density gradient as there is for the lower dynamic pressure, higher ionopause cases (see Figure 5a). This is consistent with the connection between low and thick ionopauses discussed previously by Elphic et al. [1981]. The "shoulder" in the density profile near 220 km altitude is a persistent property near the altitude where the thermal pressure first becomes equal to the magnetic pressure. This feature may be related to the large-scale ionospheric magnetic field occurring at these times [cf.

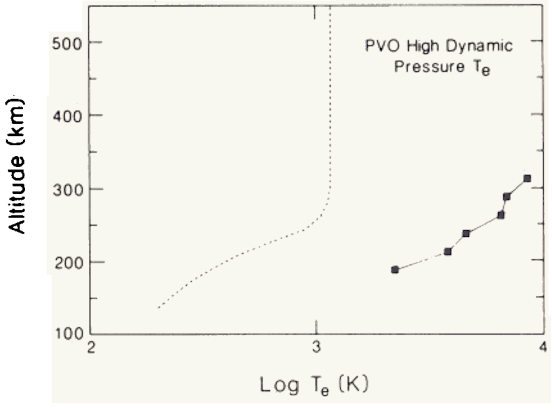

Fig. 8. Comparison of the median electron temperature for high dynamic pressure with that obtained from the model of Cravens et al. [1979] for EUV heating only.

Cravens et al., 1984]. The median electron temperature profiles (Figure 7c) show that high electron temperatures are produced at lower altitudes when the limiting ionosphere occurs. This can in some sense be attributed to the presence of the ionopause where enhanced electron temperatures are usually measured.

Figure 8 compares the electron temperature profile for high dynamic pressures with the model electron temperature computed by Cravens et al.

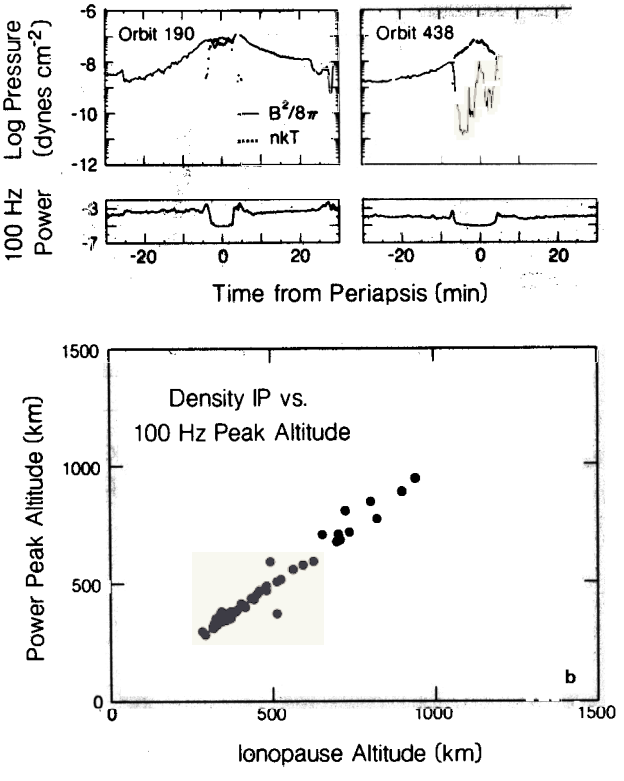

Fig. 9. (a) Examples of 100-Hz plasma wave data from Pioneer Venus, and the corresponding magnetic and thermal pressure measurements showing the local maximum in the wave power at the ionopause. (b) Comparison of the location of the 100-Hz peak with the density ionopause altitude.

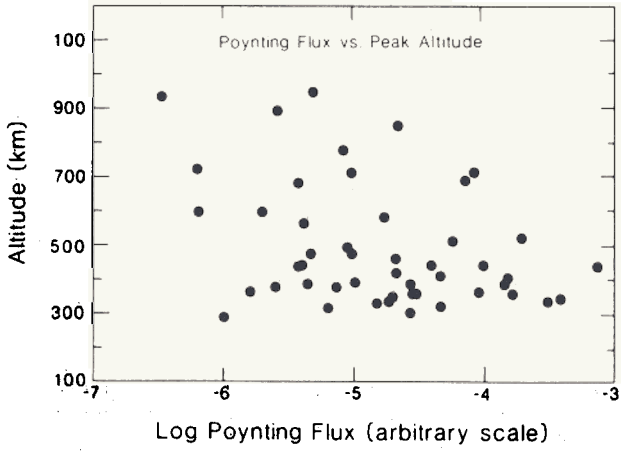

Fig. 10. Poynting flux associated with the 100-Hz peak versus the altitude of the peak power.

[1979] under the assumption of solar EUV heating alone. It was suggested in their discussion, and again in a later report [Cravens et al., 1980], that even under average conditions both magnetic field effects on the heat conductivity and an energy influx at the topside are required to obtain profiles resembling those observed. A possible topside energy source was identified in the ~100-Hz plasma waves detected on the Pioneer Venus Orbiter near the ionopause. Figure 9 illustrates the close relationship between the local maximum in the wave power at 100 Hz and the altitude of the maximum electron density gradient. However, this correlation proves neither that the waves are generated at the ionopause, nor that they are the source of heating of the electrons. The plasma waves may be generated either locally or upstream at the bow shock or in the magnetosheath. In the latter case the propagation characteristics produce the apparent maximum power at the ionopause. Taylor et al. [1979] had first pointed out that if these are indeed whistler mode waves, they are likely to be Landau damped by the ionospheric electrons which are in turn heated. The estimated energy available from this source is of the same order ($\sim 10^{9}$ eV cm^{-2} s^{-1}) as was required to model the average electron temperature profiles [Cravens et al., 1980]. Under the assumption that these waves are electromagnetic, Figure 10 compares the Poynting flux [cf. Taylor et al., 1979], which is approximately proportional to the electric field peak power multiplied by the square root of the local ionospheric plasma density (representing the index of refraction), with the altitude where the peak 100-Hz electric field power was observed. There is no clear relationship between the heating potential of the waves (e.g., the Poynting flux) and the altitude of the ionospheric boundary. Although there is an increase of the median wave Poynting flux with decreasing altitude, it is less than the event to event variation. Thus the plasma wave effects on the electron tempera-

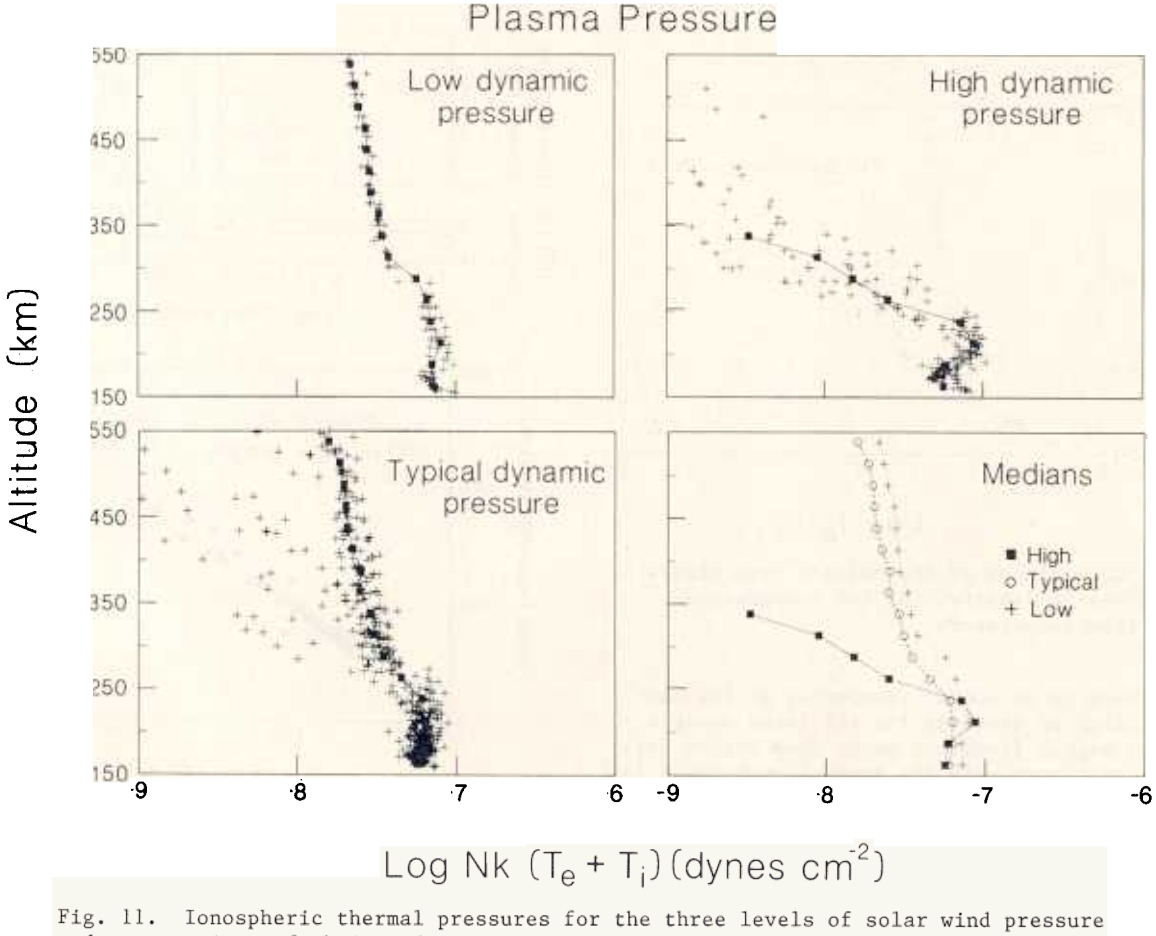

Fig. 11. Ionospheric thermal pressures for the three levels of solar wind pressure and a comparison of their medians.

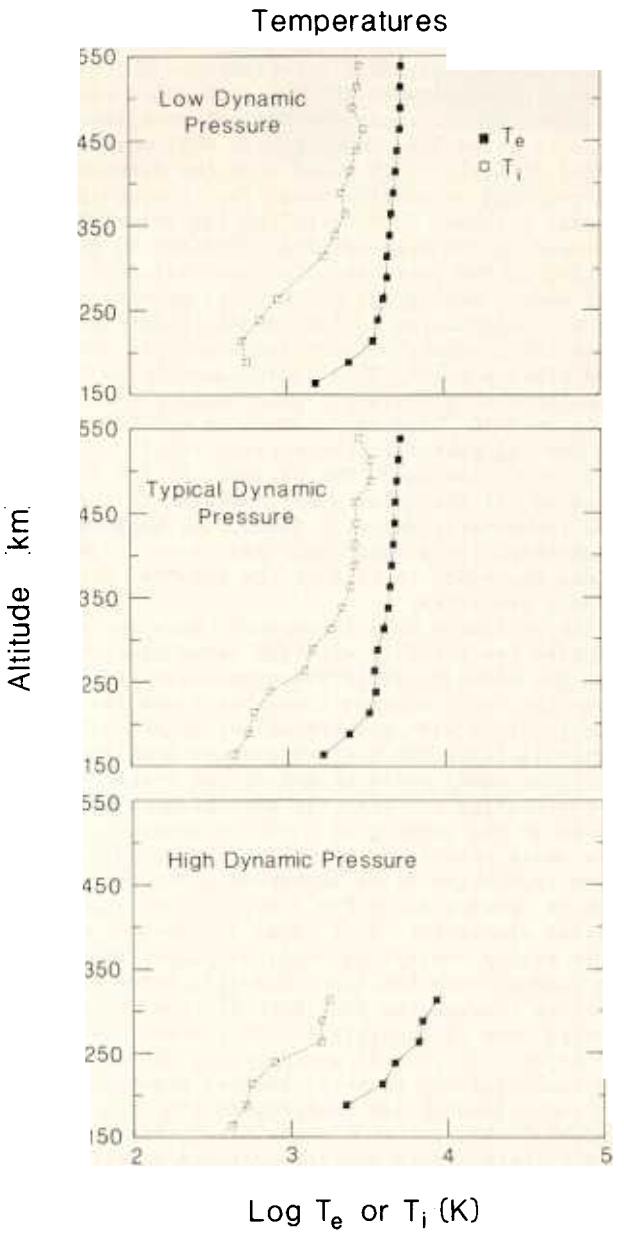

Fig. 12. Comparisons of electron and ion temperatures for the three levels of solar wind pressure.

tures are not extraordinary for the overpressure situation.

Regardless of the fact that the amount of topside heating apparently does not increase when the ionopause height is low, it is important to take into consideration the observation that the electron temperature enhancement associated with the topside heat source occurs at much lower altitudes on occasions when the minimum ionosphere is present. As Figure 11 shows, when combined with the higher local electron densities at the lower altitudes, this temperature enhancement produces a local maximum in the thermal pressure at ~ 220 km. This maximum can exceed the usual ionosphere peak pressure (by ~ 30%) and thereby alter the apparent strength of the ionospheric obstacle to the solar wind. Of course, this assessment of the pressure presumes that the Langmuir probe measurement of electron temperature in the density gradient is accurate. It is also interesting to note that the electron temperature to ion temperature ratio at the altitude of the ionopause density gradient is different from its value throughout most of the body of the ionosphere. Figure 12 compares the electron and ion temperature median altitude profiles. Whereas the ratio in the middle ionosphere is ~ 2 for low to medium dynamic pressure, it increases to ~ 3-4 below ~250 km. The high electron temperatures near the ionopause make this high ratio almost constant throughout the ionosphere for the high dynamic pressure situation. In other words, the appropriate temperature ratio to use for the pressure peak is actually greater by a factor of ~ 2 than that used to evaluate the ionospheric pressure at Mars.

While the aforementioned alteration of the ionospheric pressure profile implies that there is an ionospheric buffer to the solar wind for situations of marginal overpressure, its associated peak thermal pressure enhancement (to ~ 9×10^{-8} dyn cm^{-2}) is still sometimes exceeded by the solar wind dynamic pressure. The quantity that appears to provide the next line of defense is the magnetic field. Slavin and Holzer [1982] considered that the magnetic field contribution to the total ionospheric pressure should not exceed ~ 100%. Yet, an earlier study of the ionospheric field dependence on solar wind dynamic pressure [Luhmann et al., 1980] suggested that the ionospheric field strength increased steadily with the external dynamic pressure without any asymptotic upper limit.

The response of both the lower ionosphere thermal pressure and magnetic pressure to solar wind dynamic pressure is illustrated by Figure 13. Figure 13a shows that the thermal pressure is insensitive to the solar wind, except for the enhancement at the ionopause density gradient described above. The thermal pressure is determined, for the most part, by the neutral density, photochemistry and the solar EUV flux. Figures 13b and 13c show respectively the magnetic pressure and the sum of the magnetic and thermal pressures. As these figures indicate, the magnetic pressure in the deep ionosphere rises to match the solar wind dynamic pressure over the range of solar wind dynamic pressures occurring at Venus. The magnetic field is thus the ultimate factor in standing off the solar wind in the overpressure limit of the solar wind interaction, and the total pressure in the ionospheric plasma at Venus is never exceeded (at least in steady state) by the solar wind dynamic pressure.

From the observations, it is apparent that under ordinary circumstances, the shielding current within the ionopause increases as needed to keep the obstacle field-free except for the flux ropes and the large-scale field that the diffusion/convection mechanism supplies. However, one must consider what happens to these currents once the minimum ionosphere condition is reached and the solar wind dynamic pressure continues to grow. At first, the ionospheric vertical velocity, which, together with diffusion, is responsible for the downward transport of magnetic flux from the overlying magnetosheath, may adjust "self-consistently" in order to keep the ionospheric field sufficient to balance the external dynamic

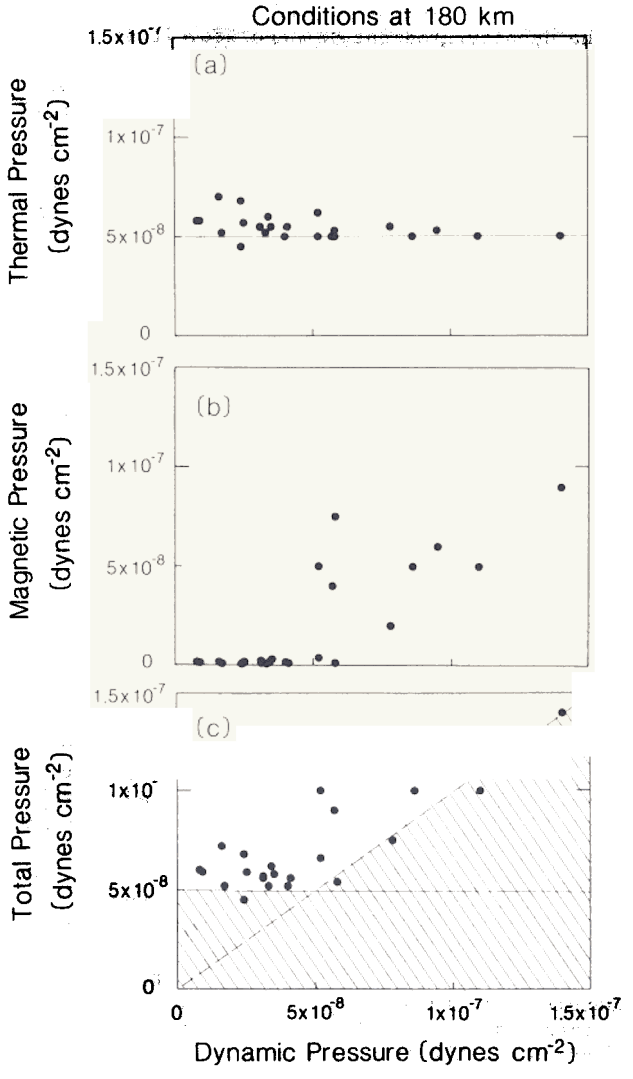

Fig. 13. (a) Subsolar ionospheric thermal pressure at 180 km for a range of incident solar wind dynamic pressures showing the constancy of the lower ionosphere. (b) Subsolar ionospheric magnetic pressure at 180 km for the data points in Figure 13a. The magnetic pressure rises to meet the solar wind pressure after the ionosphere peak pressure is exceeded. (c) Total pressure from Figures 13a and 13b illustrating the change of the dominant contribution from thermal to magnetic pressure as the dynamic pressure exceeds the former.

pressure. This can occur without substantial absorption of solar wind plasma because the "absorbed" magnetosheath flux tubes electromagnetically connect the ionosphere with the flowing magnetosheath plasma. Thus, the solar wind plasma can continue to be deflected around the obstacle of the combined planetary ionosphere and its imbedded magnetic field while driving the ionospheric convection pattern that maintains the ionospheric magnetic field. For all practical purposes, the solar wind interaction still behaves as usual except that the shielding currents are no longer confined to the collisionless part of the ionosphere.

Comparison With Mars

The above analysis of observations at Venus under conditions when the incident solar wind dynamic pressure exceeds the nominal peak ionosphere pressure gives some insight into what may be happening at Mars. It is found that the Venus obstacle responds in several ways. The ionospheric thermal pressure "perceived" by the solar wind is enhanced in the high-altitude gradient by the heating of the local electron population by whistler waves, and by the presence of generally higher temperatures in the low-altitude region where the boundary between ionosphere and solar wind plasmas forms. This enhancement helps Venus' ionosphere to withstand a solar wind pressure of up to $\sim 9\times10^{-8}$ dyn cm^{-2}, which is $\sim$30% above the nominal peak ionosphere pressure of $\sim 5.7\times10^{-8}$ dyn cm^{-2}. The ultimate factor in standing off the solar wind, however, is the dayside ionospheric magnetic field. The subsolar ionospheric field apparently adapts to achieve values necessary to balance the observed external dynamic pressures.

The available Mars ionospheric data can now be compared specifically with the Venus observations from the solar wind overpressure cases. Figure 14 shows the Venus minimum ionospheric density profile together with the Viking Mars profiles, while Figure 15 shows the ion temperature profiles for both. The small scale height of the upper portion of the density profiles for both planets is similar as is the absence of a sudden change in topside scale height. Such small scale heights may be an indication of an ionospheric density profile that is determined by the density profile of the neutral atmosphere. Horizontal ionospheric magnetic fields inhibiting vertical plasma transport can produce such behavior. The difference in the absolute ionospheric densities at these planets results from their different distances from the sun as well as from differences in the densities and constitutions of their neutral atmospheres. The comparison of ion temperature profiles in Figure 15 illustrates how the measurements at both planets exceed the temperatures expected from solar EUV heating alone. Although there are no Mars electron temperature data to compare with

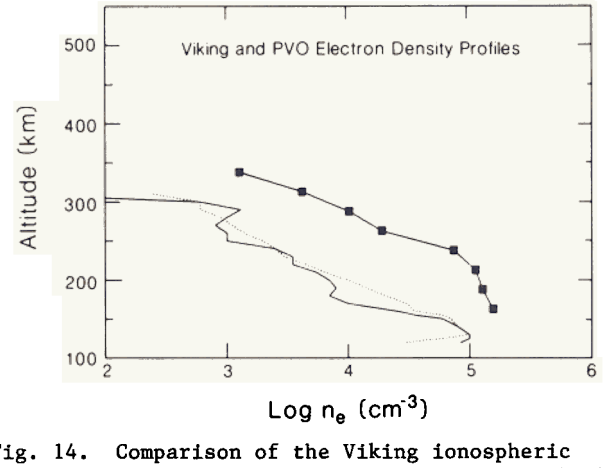

Fig. 14. Comparison of the Viking ionospheric density profile from Figure 1 with the Venus high dynamic pressure profile.

those from Venus, the electron temperature at Mars, like the ion temperature, may require a heat source beyond solar EUV (e.g., Figure 8). These data also serve as a reminder that the electron/ion temperature ratio exceeds 2 in the ionosphere for the overpressure condition at Venus.

Finally, Figure 16 displays the reported dependence of the bow shock distance at Mars on the solar wind pressure [Slavin et al., 1983]. There are far fewer points available at Mars than at Venus (see Figure 3). Nevertheless, these data show no discernible difference between the bow shock position variations at Mars and at Venus. They are equally insensitive to changes in solar wind dynamic pressures. The Martian variation also clearly does not follow the variation expected for an obstacle created by a dipolar magnetic field.

Summary and Conclusions

The response of the Venus ionosphere to the solar wind when the solar wind exceeds the peak thermal pressure in the Venus ionosphere has been characterized on the basis of observations from the Pioneer Venus Orbiter. At these times, the Venus ionosphere becomes increasingly magnetized until the total ionospheric pressure matches that of the solar wind. The ionopause becomes less distinct and asymptotically approaches a limiting altitude of about 220 km for extremely high pressures. When the ionopause is low, the hot region of electrons which occurs within the ionopause gradient extends to lower altitudes.

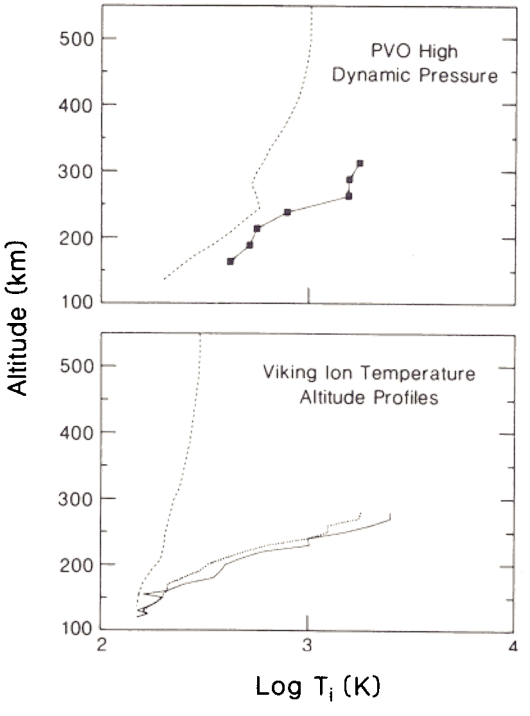

Fig. 15. Comparison of the Viking ion temperature profile with the Venus ion temperature profile. The dashed lines show the results of models with solar EUV heating alone [Chen et al., 1978; Cravens et al., 1979].

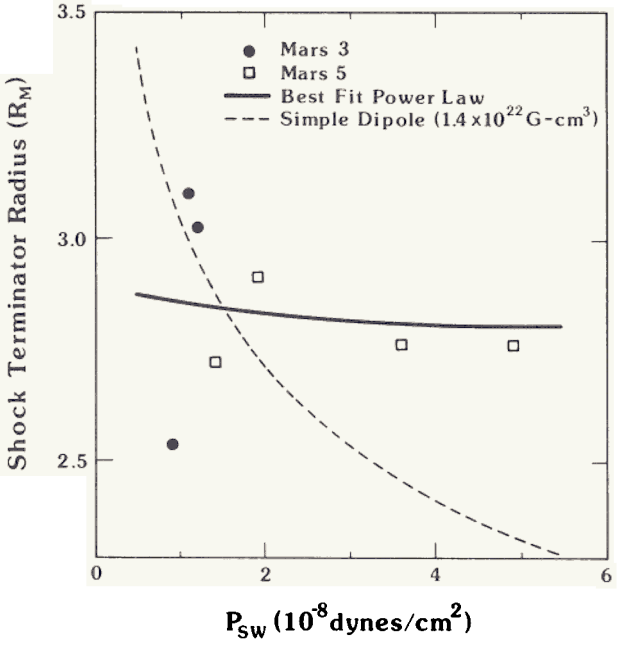

Fig. 16. Slavin et al.'s [1983] comparison of Mars bow shock positions at the terminator with the measured incident solar wind pressures. The solid and dashed lines indicate the departure of the best fit to the data from that expected for a dipole field obstacle.

The ion temperatures show little change. There is no discernable increase in plasma wave activity at the ionopause.

The limited observations from Mars compare favorably to the overpressure state of Venus. From our observations of the Venus interaction, it is seen that solar wind standoff without sufficient ionospheric plasma pressure cannot by itself be used as evidence for a planetary magnetic field. An indistinct ionopause signature is to be expected for a planet without an intrinsic field for the combined ionosphere and solar wind conditions at Mars. Furthermore, the bow shock standoff location depends on the solar wind dynamic pressure in much the same way at both Venus and Mars. Thus, we conclude that the available Mars data do not rule out the possibility that Mars is a magnetic field free obstacle to the solar wind.

Acknowledgments. This work was supported by the National Aeronautics and Space Administration under research grants NAS2-12383 and NAGW692. The solar wind data were kindly provided by J. D. Mihalov and A. Barnes of NASA Ames Research Center.

The Editor thanks R. E. Daniell and W. B. Hanson for their assistance in evaluating this paper.

References

Alexander, C. J., J. G. Luhmann, and C. T. Russell, Interplanetary control of the location of the Venus bow shock: Evidence for comet-like ion pickup, Geophys. Res. Lett., 13, 917, 1986.

Belotserkovskii, O. M., T. K. Breus, A. M. Krymskii, V. Ya. Mitnitskii, A. F. Nagy, and T. I. Gombosi, The effect of the hot oxygen corona on the interaction of the solar wind with Venus, Geophys. Res. Lett., 14, 503, 1987.

Brace, L. H., H. A. Taylor, Jr., T. I. Gombosi, A. J. Kliore, W. C. Knudsen, and A. F. Nagy, The ionosphere of Venus: Observations and their interpretations, in Venus, edited by D. M. Hunten, L. Colin, T. M. Donahue, and V. I. Moroz, p. 779, University of Arizona Press, Tucson, 1983.

Chen, R. H., T. E. Cravens, and A. F. Nagy, The Martian ionosphere in light of the Viking observations, J. Geophys. Res., 83, 3871, 1978.

Cravens, T. E., A. F. Nagy, L. H. Brace, R. H. Chen, and W. C. Knudsen, The energetics of the ionosphere of Venus: A preliminary model based on Pioneer Venus observations, Geophys. Res. Lett., 6, 341, 1979.

Cravens, T. E., T. I. Gombosi, J. Kozyra, A. F. Nagy, L. H. Brace, and W. C. Knudsen, Model calculations of the dayside ionosphere of Venus: Energetics, J. Geophys. Res., 85, 7778, 1980.

Cravens, T. E., et al., Disappearing ionospheres on the nightside of Venus, Icarus, 51, 271, 1982.

Cravens, T. E., H. Shinagawa, and A. F. Nagy, The evolution of large-scale magnetic fields in the ionosphere of Venus, Geophys. Res. Lett., 11, 267, 1984.

Dolginov, Sh. Sh., The magnetic field of Mars, Cosmic Res., Engl. Transl., 16, 204, 1978.

Elphic, R. C., and C. T. Russell, Magnetic flux ropes in the Venus ionosphere: Observations and models, J. Geophys. Res., 88, 58, 1983.

Elphic, R. C., C. T. Russell, J. G. Luhmann, F. L. Scarf, and L. H. Brace, The Venus ionopause current sheet: Thickness, length scale and controlling factors, J. Geophys. Res., 86, 11430, 1981.

Elphic, R. C., L. H. Brace, R. F. Theis, and C. T. Russell, Venus dayside ionospheric conditions: Effects of ionospheric magnetic fields and solar EUV flux, Geophys. Res. Lett., 11, 124, 1984.

Gombosi, T. I., M. Horanyi, T. E. Cravens, A. F. Nagy, and C. T. Russell, The role of charge exchange in the solar wind absorption by Venus, Geophys. Res. Lett., 8, 1265, 1981.

Hanson, W. B., S. Sanatani, and D. R. Zuccaro, The Martian ionosphere as observed by the Viking retarding potential analyzers, J. Geophys. Res., 82, 4351, 1977.

Hunten, D. M., L. Colin, T. M. Donahue, and V. I. Moroz (Eds.), Venus, University of Arizona Press, Tucson, 1983.

Johnson, F. S., and W. B. Hanson, A new concept for the daytime magnetosphere of Venus, Geophys. Res. Lett., 8, 581, 1979.

Johnson, R. E., Comment on ion and electron temperatures in the Martian upper atmosphere, Geophys. Res. Lett., 5, 989, 1978.

Luhmann, J. G., R. C. Elphic, C. T. Russell, J. D. Mihalov, and J. H. Wolfe, Observations of large-scale steady magnetic fields in the dayside Venue ionosphere, Geophys. Res. Lett., 7, 917, 1980.

Luhmann, J. G., C. T. Russell, and R. C. Elphic, Time scales for the decay of induced large-scale magnetic fields in the Venus ionosphere, J. Geophys. Res., 89, 362, 1984.

Luhmann, J. G., R. J. Warniers, C. T. Russell, J. R. Spreiter, and S. S. Stahara, A gasdynamic magnetosheath field model for unsteady interplanetary fields: Application to the solar wind interaction with Venus, J. Geophys. Res., 91, 3001, 1986.

Mihalov, J. D., J. R. Spreiter, and S. S. Stahara, Comparison of gasdynamic model with steady state solar wind flow around Venus, J. Geophys. Res., 87, 10363, 1982.

Miller, K. L., W. C. Knudsen, and K. Spenner, The steady state dayside Venus ionosphere, I, Pioneer-Venus retarding potential analyzer experimental observations, Icarus, 57, 386, 1984.

Phillips, J. L., J. G. Luhmann, and C. T. Russell, Growth and maintenance of large-scale magnetic fields in the dayside Venus ionosphere, J. Geophys. Res., 89, 10676, 1984.

Rohrbaugh, R. P., J. S. Nisbet, E. Bleuler, and J. R. Herman, The effect of energetically produced O_2^+ on the ion temperatures of the Martian thermosphere, J. Geophys. Res., 84, 3327, 1979.

Russell, C. T., J. G. Luhmann, J. R. Spreiter, and S. S. Stahara, The magnetic field of Mars: Implications from gasdynamic modeling, J. Geophys. Res., 89, 2997, 1984.

Saunders, M. A., and C. T. Russell, Average dimension and magnetic structure of the distant Venus magnetotail, J. Geophys. Res., 91, 5589, 1986.

Shinagawa, H., T. E. Cravens, and A. F. Nagy, A one-dimensional time-dependent model of the magnetized ionosphere of Venus, J. Geophys. Res., in press, 1987.

Slavin, J. A., and R. E. Holzer, The solar wind interaction with Mars revisited, J. Geophys. Res., 87, 10285, 1982.

Slavin, J. A., et al., The solar wind interaction with Venus: Pioneer Venus observations of bow shock location and structure, J. Geophys. Res., 85, 7625, 1980.

Slavin, J. A., R. E. Holzer, J. R. Spreiter, S. S. Stahara, and D. S. Chausee, Solar wind flow about the terrestrial planets, 2, Comparison with gasdynamic theory and implications for solar-planetary interactions, J. Geophys. Res., 88, 19, 1983.

Spreiter, J. R., and S. S. Stahara, Solar wind flow past Venus: Theory and comparisons, J. Geophys. Res., 85, 7715, 1980.

Tatrallyay, M., C. T. Russell, J. D. Mihalov, and A. Barnes, Factors controlling the location of the Venus bow shock, J. Geophys. Res., 88, 5613, 1983.

Taylor, W. W. L., F. L. Scarf, C. T. Russell, and L. H. Brace, Absorption of whistler mode waves in the ionosphere of Venus, Science, 205, 112, 1979.

Theis, R. F., L. H. Brace, and H. G. Mayr, Empirical models of the electron temperature and density in the Venus ionosphere, J. Geophys. Res., 85, 7787, 1980.

Vaisberg, O., and V. Smirnov, The Martian magnetotail, Adv. Space Res., 6, 301, 1986.

L. H. Brace, NASA Goddard Space Flight Center, Code 614, Greenbelt, MD 20771.

W. C. Knudsen, Knudsen Geophysical Research, Monte Sereno, CA 95030.

J. G. Luhmann and C. T. Russell, Institute of Geophysics and Planetary Physics, University of California, Los Angeles, CA 90024.

F. L. Scarf, TRW, Building R-1, Room 1176, One Space Park, Redondo Beach, CA 90278.

(Received February 17, 1987;
revised April 7, 1987;
accepted April 28, 1987.)